Presented at COMSOL Conference 2020

FINITE ELEMENT MODELING OF AN ALGAN/GAN BASED VOC SENSOR USING COMSOL

Balaadithya Uppalapati[1], Akash Kota[2], Vamsy P. Chodavarapu[2], Goutam Koley[1]

[1]Department of Electrical & Computer Engineering, Clemson University, Clemson, SC, USA
[2]Department of Electrical & Computer Engineering, University of Dayton, Dayton, OH, USA

Outline

- Introduction
- Geometry Setup
- Simulation Procedure
- Results
- Summary

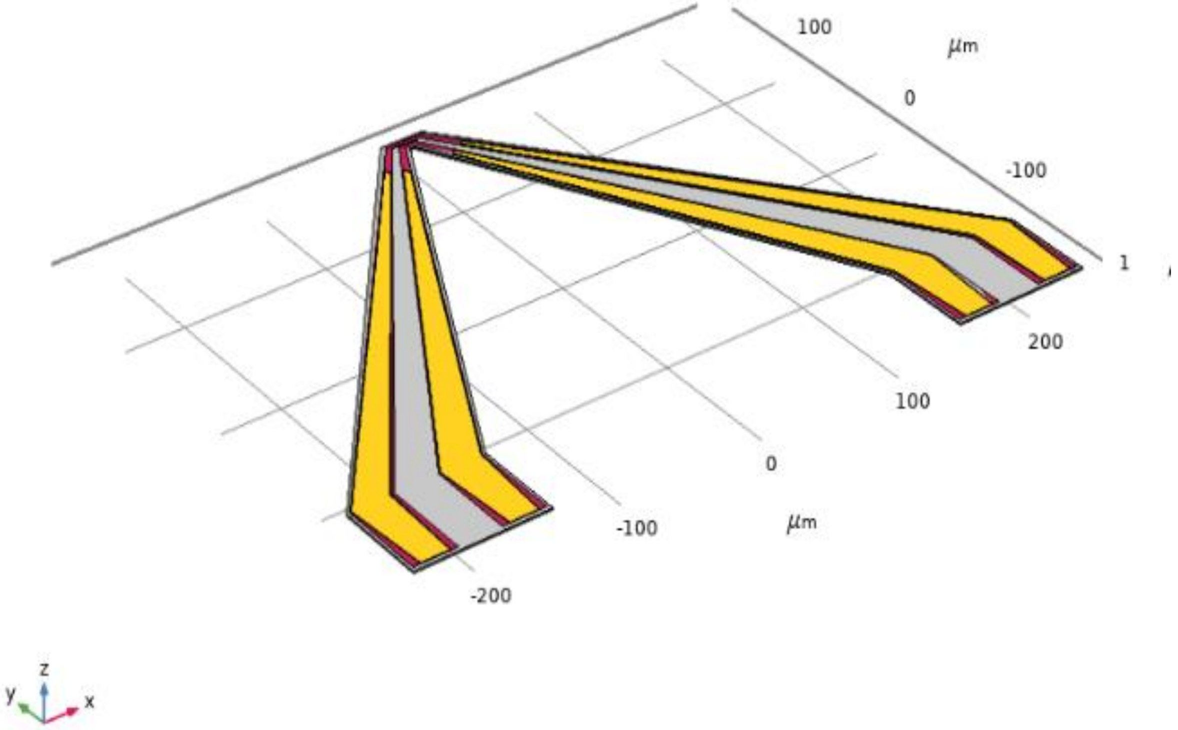

Introduction

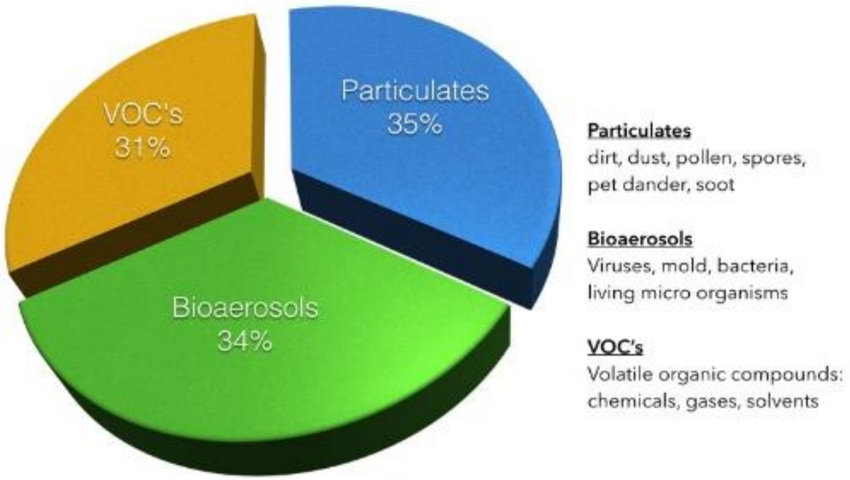

Source: H. Guo *et. al.*, Environ. Res. 94 (1), 57-66 (2004)

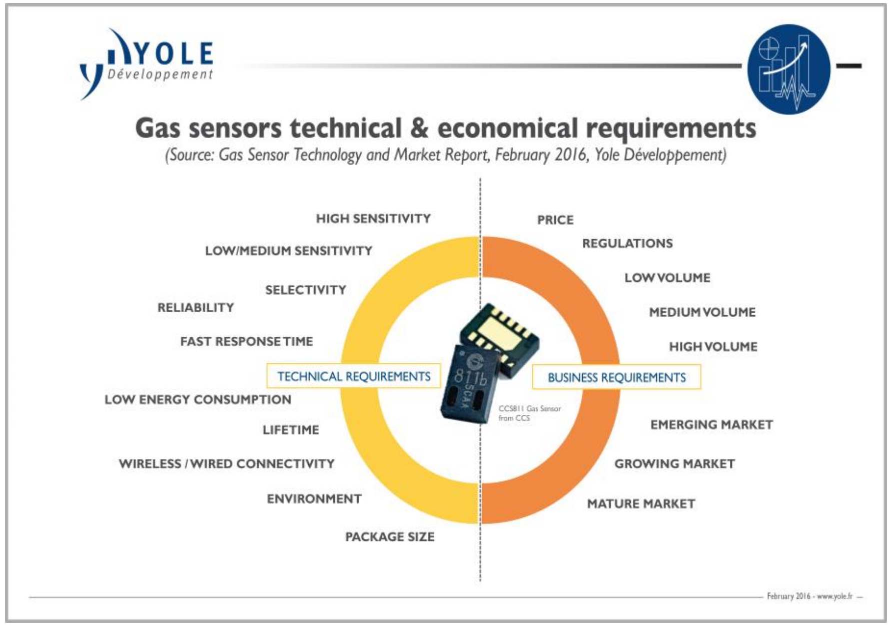

Source: Yole Developpement

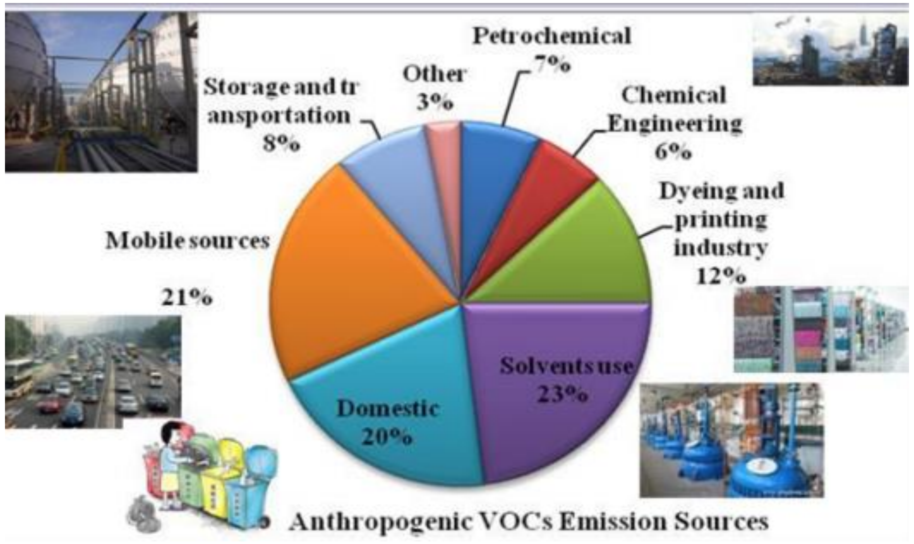

Source:https://www.healthypeople.gov/2020/topics-objectives/topic/respiratory-diseases

- An AlGaN-GaN-AlGaN based dual channel microcantilever has been simulated to compute the temperature profiles
- Using the electric currents (ec) module, the electric field intensity, current density and the electromagnetic loss profiles of the cantilever are computed
- By coupling the ec module with heat transfer (ht) module, the temperature profiles are obtained

Geometry Setup

3D Geometry of the AlGaN-GaN-AlGaN dual channel micro cantilever

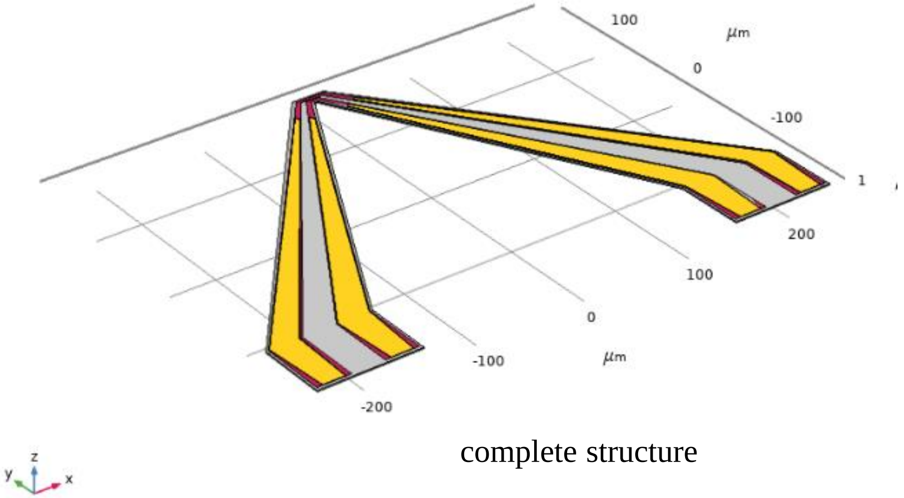

complete structure

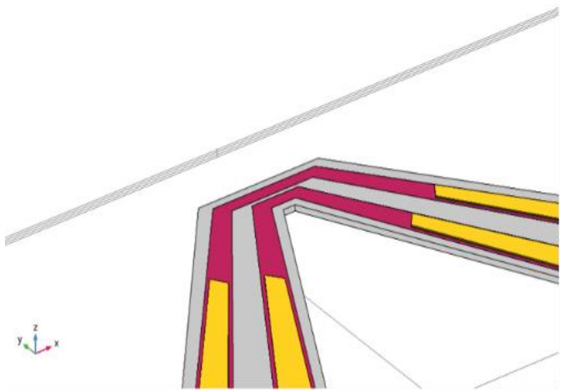

the tip region

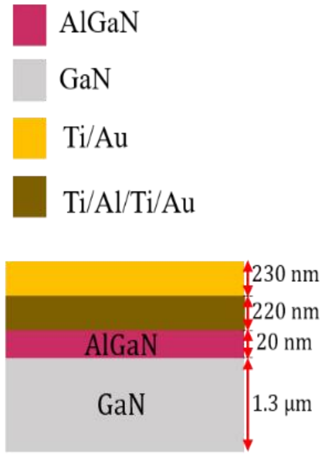

- To compute the temperature profiles of the cantilever at different bias voltages the required material properties are
  - ➢ electrical conductivity (σ),
  - ➢ relative permittivity (ϵ_r),
  - ➢ thermal conductivity (k),
  - ➢ density (ρ)
  - ➢ heat capacity at constant pressure (c_p)

Table 1 illustrates the properties of all the materials used in the simulation

	GaN	AlGaN	Metal stack 1	Metal stack 2
σ (S/m)	1695	96154	2.6e6	2.6e6
ϵ_r	9.5	8.9	1	1
(W/(m. K)	41	52.7	21.9	317
ρ(kg/m^3)	6150	5740	4506	19300
$_p$(J/(kg. K)	490	490	522	129

Simulation procedure

- For the given 3D geometry, the temperature profiles at different bias voltages are computed using the electric currents (ec) and heat transfer (ht) modules

- Using the ec module, electric potential boundary conditions are used to apply the bias voltages on the inner channels
  - For instance, in this simulation DC bias voltages such as 10 V and 0 V are applied on the edge boundaries of the gold layers located at the left and right arms of the cantilever base region respectively

- From the electric potential (V), the profiles of electric field intensity (E), current density (J), and electromagnetic losses (Q_e) are computed

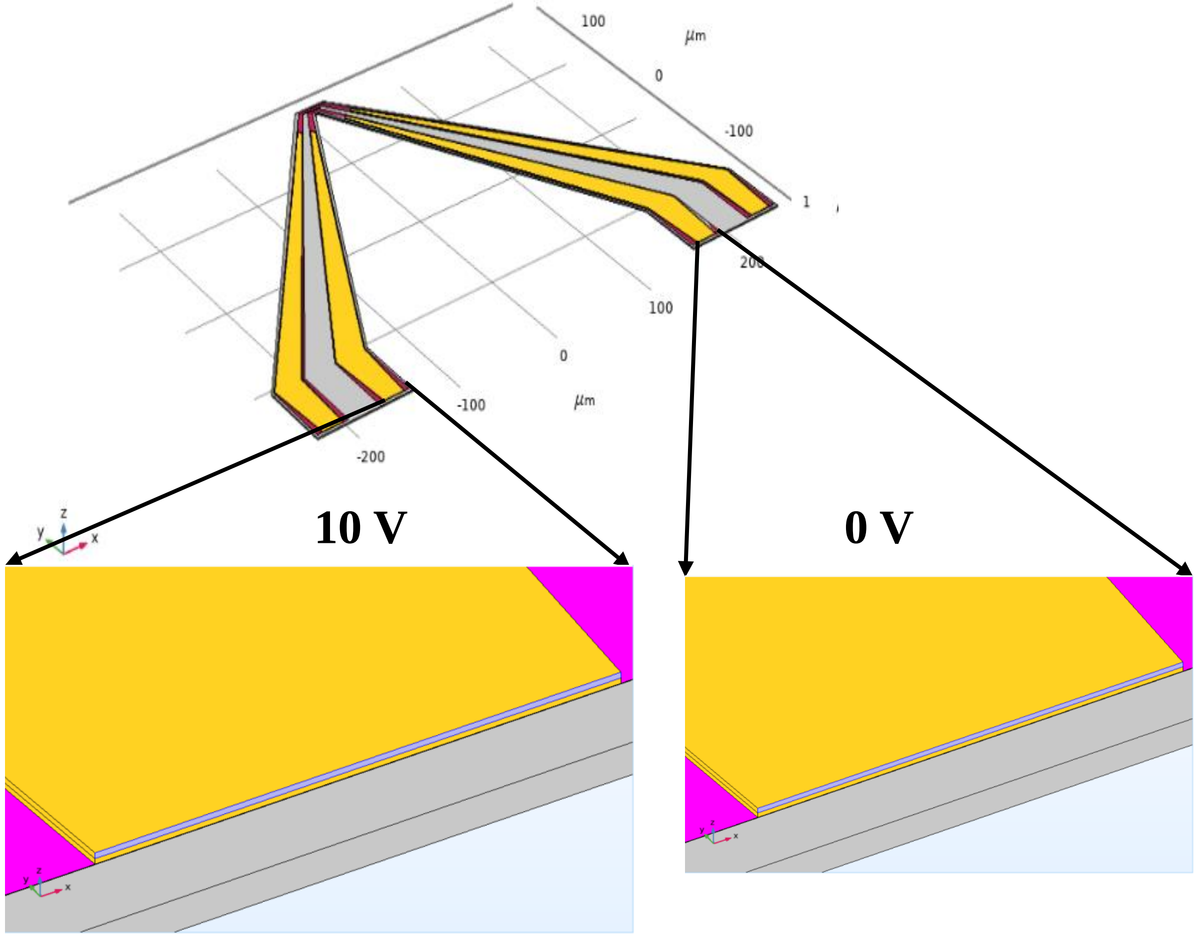

Simulation procedure cont.…

$$E = -\nabla V, \qquad (1)$$

$$J = \sigma . E, \qquad (2)$$

$$\nabla . J = Q_e . \qquad (3)$$

The electromagnetic loss data obtained from the ec module is given as input to the ht module to solve the heat equation which can be written as

$$(\rho \cdot c_p \cdot \vec{u}) \cdot \nabla T = \nabla \cdot (\vec{q}) + Q_e, \qquad (4)$$

where $$\vec{q} = k \cdot \nabla T. \qquad (5)$$

In Eq. (4) $\vec{u}$ is the fluid velocity vector, T is the temperature and $\vec{q}$ is the conductive heat flux. Convective and radiative heat losses are also considered in the simulation. The equation to represent the convective heat loss can be written as

$$-\vec{n} \cdot \vec{q} = q_0, \qquad (6)$$

where $$q_0 = h \cdot (T_{ext} - T). \qquad (7)$$

The equation to compute the radiative heat loss can be written as

$$-\vec{n} \cdot \vec{q} = \varepsilon \cdot \sigma \cdot (T_{amb}^4 - T^4), \qquad (8)$$

Electric Field Intensity profile

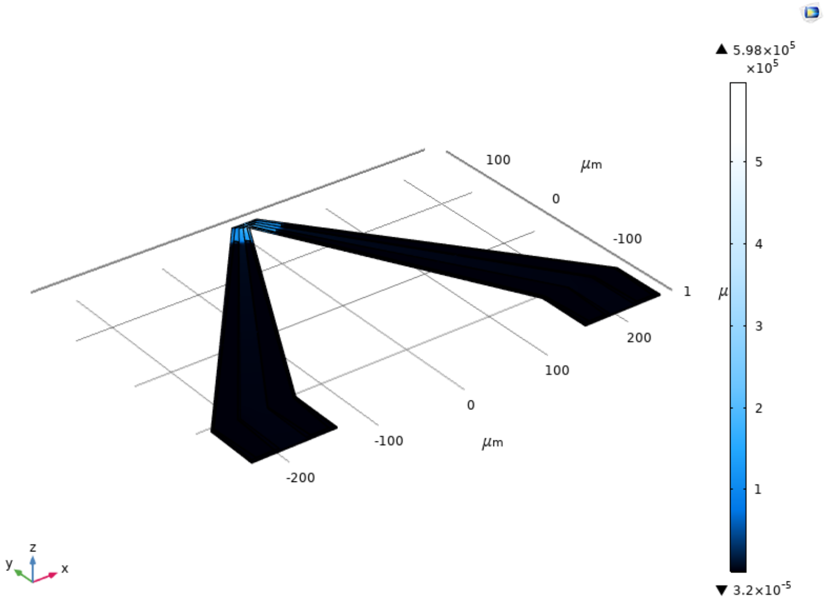

At bias voltage of 10 Volts

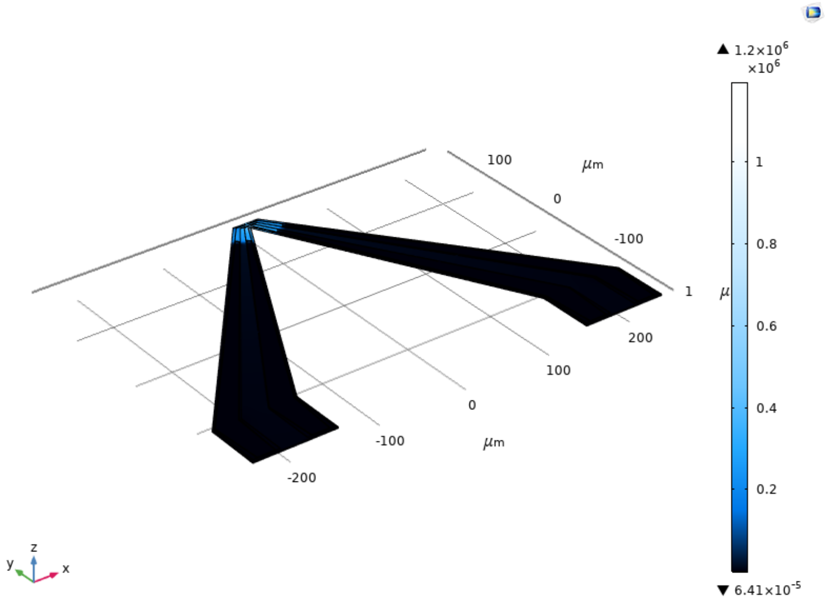

At bias voltage of 20 Volts

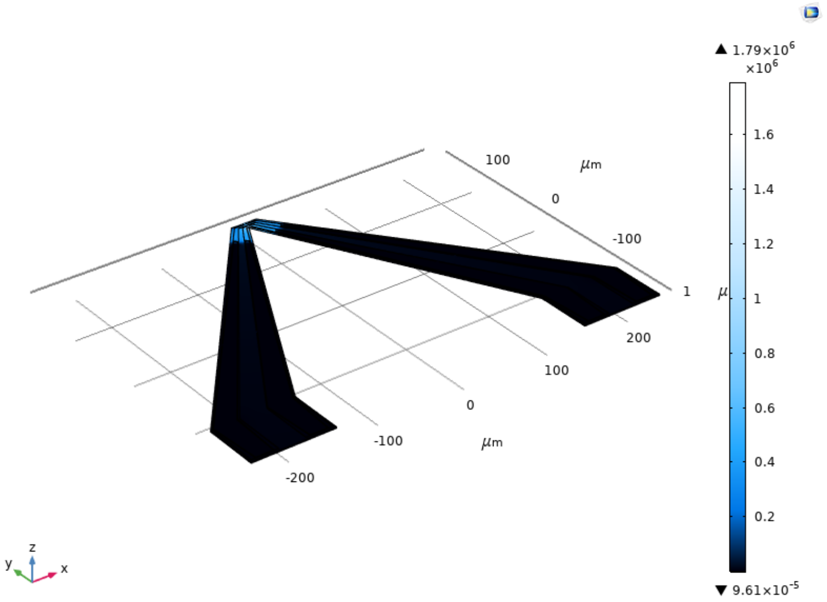

At bias voltage of 30 Volts

Temperature Profile

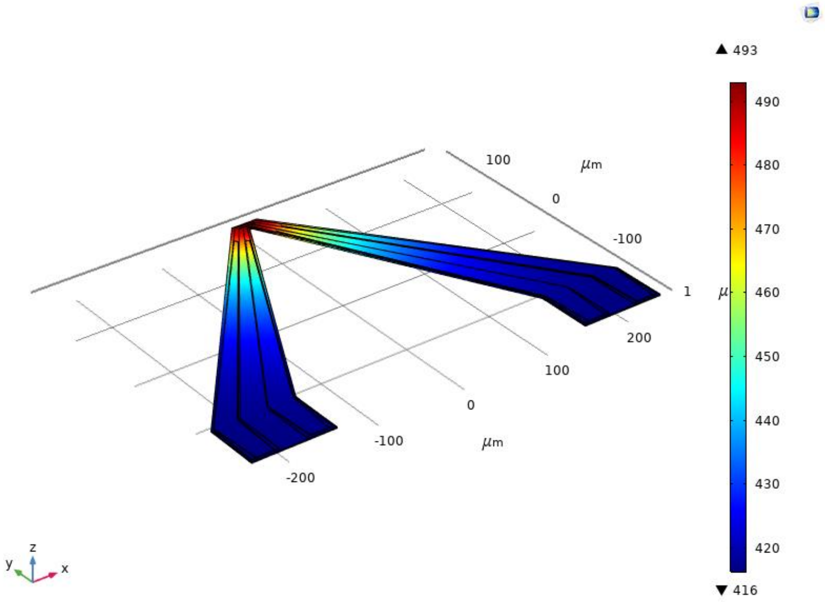

At bias voltage of 10 Volts

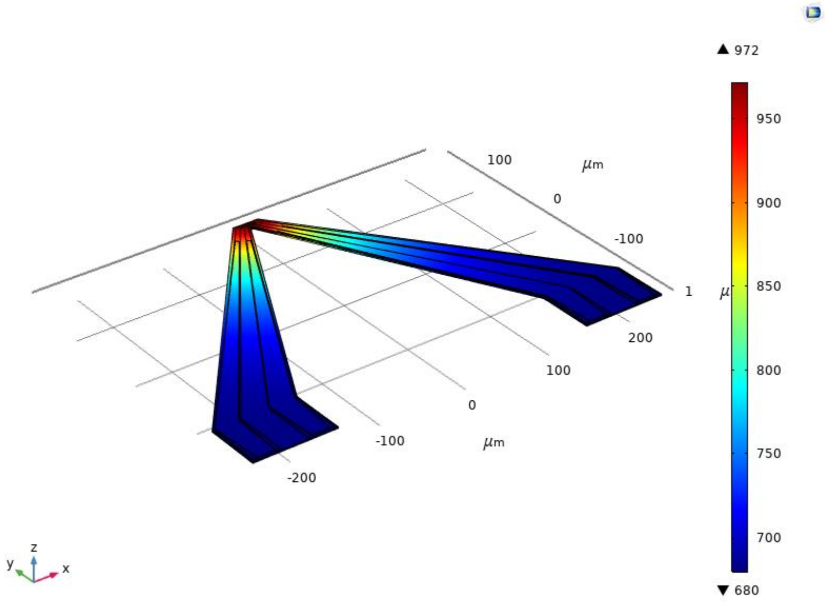

At bias voltage of 20 Volts

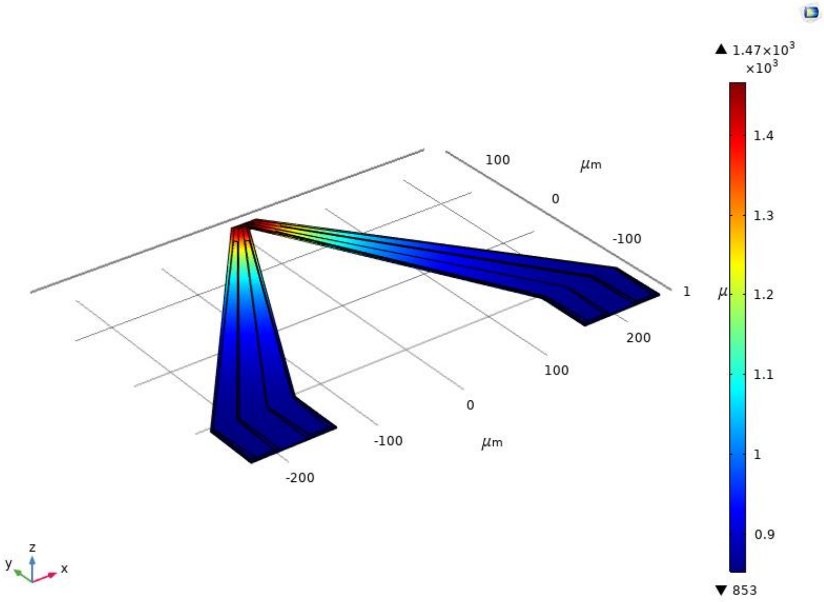

At bias voltage of 30 Volts

Conclusion

- An AlGaN-GaN-AlGaN based dual channel cantilever has been simulated in COMSOL to obtain the temperature profiles at different DC bias voltages
- To perform the simulations the electric currents and heat transfer modules are coupled
- The DC bias voltages are varied from 5 V to 30 V with a step size of 5 V
- From the simulation results, it can be concluded that at every bias voltage the magnitude of electric field intensity and temperature is maximum at the tip region of the cantilever
- Also, as the applied bias voltage increases, the electric field intensity and temperature also increases
- The numerical results obtained from these simulations are useful for validating the experimental results

References

1. J.T. Brinke *et.al*, “Development of new volatile organic compound (VOC) exposure metrics and their relationship to sick building syndrome symptoms,” *Indoor Air*, **8**, 140–152 (1998).
2. P.S. Burge, “Sick building syndrome,” *Occup. Environ. Med.*, **61**, 185–190 (2004).
3. World Health Organization, “WHO Guidelines for Indoor Air Quality: Selected Pollutants,” Geneva (2010). Available online:http://www.euro.who.int/__data/assets/pdf_file/0009/128169/e94535.pdf.
4. H. Guo, S.C. Lee, L.Y. Chan, and W.M. Li, “Risk assessment of exposure to volatile organic compounds in different indoor environments,” *Environ. Res.*, **94**, 57–66 (2004).
5. Y. Zhou *et.al*, “Application of portable gas chromatography-photo ionization detector combined with headspace sampling for field analysis of benzene, toluene, ethylbenzene, and xylene in soils,” *Environ. Monit. and Assess.*, **185**, 3037– 3048 (2013).
6. L. Spinelle *et al.*, “Review of Portable and Low-Cost Sensors for the Ambient Air Monitoring of Benzene and Other Volatile Organic Compounds,” *Sensors*, **17**, 1520 (2017).
7. J.S. Kim, H.W. Yoo, H.O. Choi, and H.T. Jung, “Tunable volatile organic compounds sensor by using thiolated ligand conjugation on MoS2,” *Nano Lett.*, **14**, 5941–5947 (2014).
8. B. Buszewski *et al.*, “Analysis of exhaled breath from smokers, passive smokers and nonsmokers by solid phase microextraction gas chromatography/mass spectrometry,” *Biomed. Chromatogr.*, **23**, 551–556 (2009).
9. A. B. Kanu *et al.*, “Ion mobility–mass spectrometry,” *Int. J. Mass Spectrom.* , **43**, 1-22 (2008).
10. C.D Natale *et al.*, “Lung cancer identification by the analysis of breath by means of an array of non-selective gas sensors,” *Biosens. Bioelectron*., **18** 1209–1218 (2003).
11. I. Elmi *et al.*,“Development of ultra-low-power consumption MOX sensors with ppb-level VOC detection capabilities for emerging applications,” *Sens. Actuators B Chem.*, **135**, 342-351 (2008).
12. N. Tang, Y. Jiang, H. Qu, and X. Duan “Conductive polymer nanowire gas sensor fabricated by nanoscale soft lithography,” *Nanotechnology*., **28**, 485301 (2017).
13. N. Tang *et al.*, “A fully integrated wireless flexible ammonia sensor fabricated by soft nano-lithography,” *ACS Sensors*., **4**, 726–732 (2019).
14. J.W. Grate *et al.*, “Smart sensor system for trace organophosphorus and organosulfur vapor detection employing a temperature-controlled array of surface acoustic wave sensors, automated sample preconcentration, and pattern recognition,” *Analytical Chemistry*, **65**, 1868–1881 (1993).
15. J. Getino, J *et al.*, “Analysis of VOCs with a tin oxide sensor array,” *Sens. Actuators B Chem.*, **43**, 200–205 (1997).
16. W. Zhang *et al.*, “Ultrafine Tungsten Oxide Nanowires: Synthesis and Highly Selective Acetone Sensing and Mechanism Analysis,” *ACS Appl. Mater. Interfaces*, **12**, 3755-3763 (2019).
17. S.G. Leonardi, “Two-dimensional zinc oxide nanostructures for gas sensor applications,” *Chemosensors*, **5**, 17 (2017).
18. O.Lupan *et al.*, “Single and networked CuO nanowires for highly sensitive p-type semiconductor gas sensor applications,” *physica status solidi (RRL)–Rapid Research Letters*, **10**, 260–266 (2016).
19. T.J. Flack, B.N. Pushpakaran, and S.B. Bayne, “GaN Technology for Power Electronic Applications: A Review,” *J. Electron. Mat.* , **45**, 2673–2682 (2016).
20. G. Simin *et al.*, “III-nitride microwave control devices and ICs,” *Semiconductor Science and Technology*, **28**, 74008 (2013).
21. M. Stutzmann *et al.*, “GaN-based heterostructures for sensor applications,” *Diamond and Related Materials*, **11**, 886–991 (2002).
22. M. Rais-Zadeh *et al.*, “Gallium Nitride as an Electromechanical material,” *J. Microelectomech. Syst.*, **23**, 1252–1271 (2014).
23. I. Jahangir, E.B. Quddus, and G. Koley, “Unique detection of organic vapors below their auto-ignition temperature using III–V Nitride based triangular microcantilever heater,” *Sens. Actuators B Chem.*, **222**, 459-467 (2016).
24. S. Gorman, D. Gajula, S. Kim and G. Koley, “Impact of volatile organic compound exposure on electrical breakdown in GaN dual channel microcantilevers,” *Appl. Phys. Lett.*, **114**, 114103, (2019).
25. N. DeRoller, M. Qazi, J. Liu, and G .Koley, “Characterization of an AlGaN/GaN electrostatically actuated cantilever using Finite Element Method,” in *Proc. COMSOL conf.*, Boston (2010).